Materials Science-Poland, *Vol. 27*, *No. 3*, *2009*

Magnetic properties of mechanically milled nanosized Mn

X.J. WU[1*], X.W. XU[1], X.S. SUN[2]

[1]Material Science & Technology College, Shenyang Ligong University, Shenyang 110168, China

[2]College of Materials & Metallurgy, Northeastern University, Shenyang 110006, China

Nanosized Mn powders were fabricated by milling Mn flakes in pure ethyl alcohol followed by homogenization. XRD analysis confirms single-phase characterization of the product and shows it has a grain size of 40 nm. The ZFC and FC magnetizations exhibit a large irreversibility with onset of about 60 K. The fit of the Curie–Weiss relation indicates strong AFM interaction in the considered system. A large coercive field and shifted hysteresis loops, i.e. H_e = 83.6 kA/m, are observed at 5 K in the 2 T field cooling case. The analysis indicates that surface anisotropy can lead to the occurrence of large exchange bias.

Key words: *nanosized powder; exchange bias; antiferromagnetism; surface anisotropy*

1. Introduction

Antiferromagnetic nanoparticles (AFN) have recently received increased attention due to their potential for exhibiting magnetization reversal by quantum tunnelling [1, 2]. Large surface to volume ratios of AFN make it reasonable to correlate their magnetic behaviours with surface effects. AFN such as NiO and CuO exhibited the exchange bias effect (EB) and a hysteresis loop, which indicates the existence of strong inter-particle interactions [3, 4]. Typically, these effects occur when the ferromagnetic (FM)–antiferromagnetic (AFM) interface is cooled through the Néel temperature (T_N) of the AFM in the field-cooled case. Besides, the exchange bias is known to enhance the coercivity and the shift of the hysteresis loop along the field axis [5]. Meiklejohn and Bean observed exchange anisotropy in core-shell Co/CoO nanoparticles, where the FM Co core was oxidized to produce an AFM CoO shell [6]. On the other hand, AFN can serve as a natural candidate material for the study of exchange bias, in which the core is AFM and the shell is FM, based on its high concen-

*Corresponding author, e-mail: wu_xiaojuan@yahoo.com.cn

tration of surface defects. The occurrence of the exchange bias field in CuO AFN was ascribed to the exchange interaction between surface defects, resulting from the increase in the surface area of the nanoparticles upon size reduction, and the AFM core [7]. If the presence of defects has a role in exchange bias, further enhancement in the exchange bias field is possible via mechanical milling, i.e. the process which introduces large defects on the surface of the particles from plastic deformation and size reduction.

Among the 3d transition metal elements, Mn can be considered as the most complex of all metallic elements. Due to possessing a moment as high as 5 μB, Mn and various structures containing Mn are expected to exhibit a variety of magnetic properties. In the past two decades, considerable interest in Mn nanostructures has been devoted to theoretical studies and experimental investigations [8]. Irrespective of the fact that nanosized particles of other transition metals have been extensively studied [9], reports on Mn nanoparticles are comparatively rare.

In this work, nanosized Mn powders were prepared successfully by milling Mn flakes for 50 h in a pure ethyl alcohol medium, followed by homogenization. The structure and magnetic properties of the powders were investigated in detail.

2. Experimental

Mn flakes (–22 mesh, 99.99%) were milled for 50 h in a home-made planetary ball mill, with a powder-to-ball weight ratio of 1:14, and at the spin rate of 400 rpm. The powders were milled in a tungsten carbide bowl in a pure ethyl alcohol medium using tungsten carbide balls. The as-milled powders were annealed at 673 K in a high vacuum for 30 min. X-ray diffraction (XRD) patterns were obtained with a Philips PW-1404 diffractometer using CuK_α radiation. The Williamson–Hall relationship was used to calculate the effect of the grain size. The temperature and magnetic field variation of the magnetization M for the sample were measured with a vibrating sample magnetometer (VSM). In the zero-field-cooled (ZFC) case, the sample was cooled to 5 K in a zero field; a measuring field was then applied, followed by data acquisition as the temperature was increased. In the field-cooled (FC) case, the sample was cooled in a field, followed by the data acquisition as described above.

3. Results and discussion

Figure 1 represents XRD patterns of the as-annealed Mn powders. Obviously, Mn single phase is indexed with a space group of $I\bar{4}3m$. The lattice parameter a calculated from the (444) diffraction peak equals 0.8910 nm, basically consistent with the standard value of a = 0.8912 nm (Card Number: 89-4252). Moreover, all the diffraction peaks exhibit broadening, which reveals the presence of nanocrystallites. In addi-

tion, from the half-width of the XRD peaks of the pattern, the grain size is estimated as 40 nm for the nanosized Mn powders.

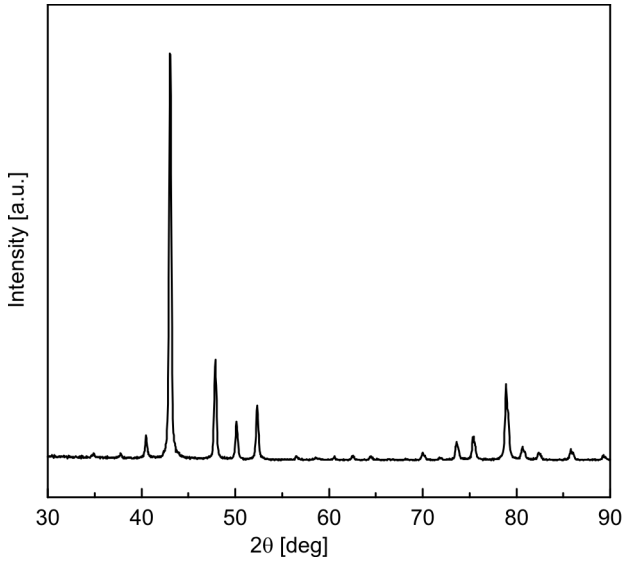

Fig. 1. XRD patterns of the nanosized Mn powders

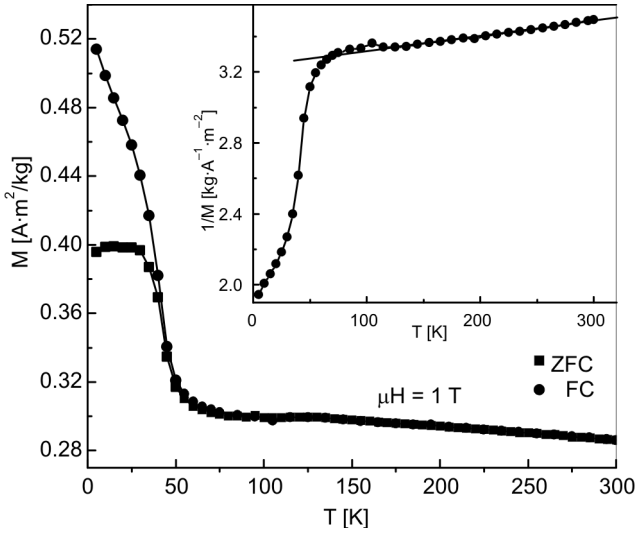

Fig. 2. Temperature dependences of zero-field cooled and field cooled magnetizations of nanosized Mn powders. Inset: Temperature dependence of reciprocal magnetization $1/M$ measured in the FC process with the field of 1 T, and the line shows that $1/M$ is fitted to the Curie–Weiss dependence for the data of $T > 50$ K

The ZFC and FC magnetizations of nanosized Mn powders, as functions of temperature under the magnetic field of 1 T, are shown in Fig. 2. The inset in this figure

shows the temperature dependence of the reciprocal magnetization, $1/M$, as measured in the FC process with the field of 1 T. As temperature is lowered from room temperature, a very sharp step at about 30 K is observed in the M_{ZFC} curve with the field of 1 T, while a gradual increase of M_{FC} appears, especially, below 50 K. Namely, an increasingly large irreversibility is observed between M_{ZFC} and M_{FC}, with the onset of about 60 K. The maximum in the ZFC curve, at about 30 K, is usually ascribed to the average blocking temperature of the magnetic moment T_B, corresponding to the largest particles in the size distribution. Assuming the measured moments are due to uncompensated surface spins, Néel [10] suggested that the spin lattice of the particle could reverse coherently and randomly under thermal activation, and that the net moment of the uncompensated surface spins would fluctuate accordingly, i.e., superparamagnetism, with a blocking temperature below which spin systems are stable. Furthermore, the fit of the Curie–Weiss relation, i.e. $\chi = C/(T - \Delta)$, as shown in the inset, gives $\Delta = 3796$ K, which reveals very strong antiferromagnetism of the nanosized Mn powders.

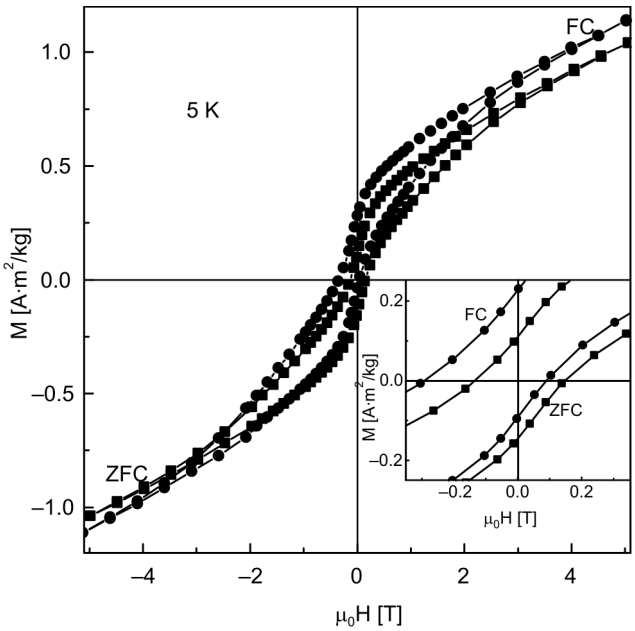

Fig. 3. The hystereis loops of nanosized Mn powders under the ZFC and FC cases. The inset shows the same loops in a larger magnification

The hysteresis loops of the nanosized Mn powders at 5 K were measured in magnetic fields up to 5 T before and after field cooling at 2 T, as shown in Fig. 3. Its inset shows the same dependences in a larger magnification. Obviously, the ZFC loop is almost symmetric around the origin, whereas the 2 T field is strongly displaced from the origin and even broadened. The value of the displacement defines directly the EB

field H_e. A large coercive field and shifted hysteresis loops, including vertical and horizontal directions, are observed after cooling in a 2 T field. Commonly, the ZFC isofield curve of the AFN can be expressed by the equation

$$M(H) = M_{\mathrm{FM}}(H) + \chi_{\mathrm{AF}} H$$

where χ_{AF} is the antiferromagnetic susceptibility of the core and N_{FM} denotes the magnetization due to uncompensated surface spins.

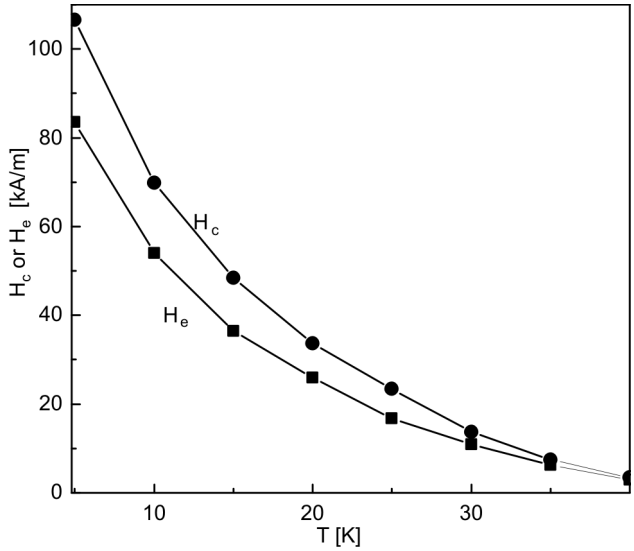

Fig. 4. Temperature dependences of exchange bias and coercive field of nanosized Mn powders

For the FC case, the temperature dependences of coercive (H_c) and exchange bias fields (H_e) are shown in Fig. 4. A maximum H_e = 83.6 kA/m can be observed at 5 K. Furthermore, both H_c and H_e decrease with the increase in temperature and both almost disappear above 50 K, the bifurcation temperature in Fig. 2a.

According to Néel [10], weak ferromagnetic behaviour from very fine antiferromagnetic particles can be attributed to the uncompensated spins on the surfaces of the particles, which has verified for a lot of AFN, such as MnO [11], Co_3O_4 [12] and CuO [13], etc. Kodama et al. [14] suggested that the reduced coordination of surface spins, resulting from the finite size effect, can cause a fundamental change in the magnetic order, which leads to large coercivity and loop shifts. In addition to surface spin canting and surface spin disorder via the synthesis techniques of ball milling, the change of coordination of the surface atoms, especially in oxides due to broken exchange bonds [15], can also render surface spin disorder. This indicates that surface anisotropy is present in the system. Moreover, nanosized particles/powders are often enclosed by a thin oxide layer, when they are exposed to air [16].

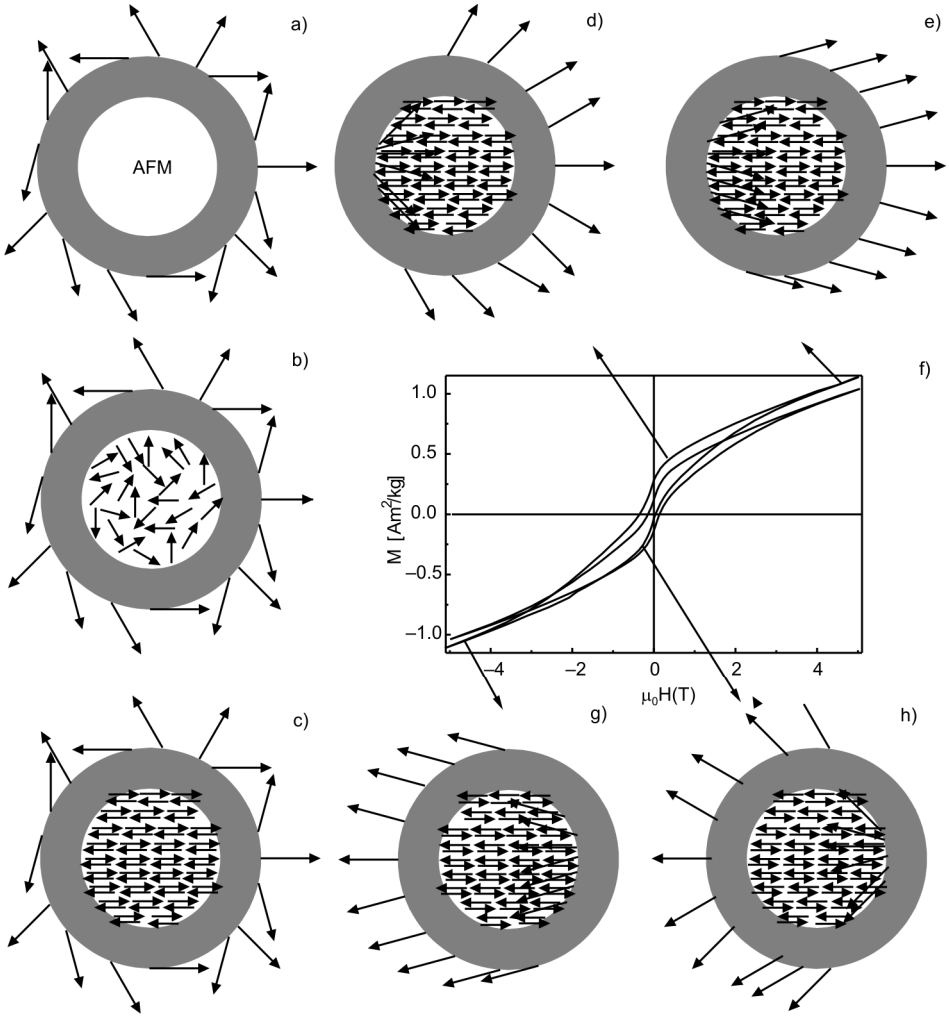

Fig. 5. The schematic diagram of the spin configurations in the nanosized Mn powders at various magnetization stages. Details in the text

A simple phenomenological model has been constructed based on the aforementioned findings to illustrate the spin configurations in the nanosized EB system (Fig. 5) [17]. Mn can form several types of oxides depending on the Mn to O ratio, which is usually controlled by the diffusion of oxygen. Therefore, we can refer to the oxide layer as Mn(O), shown as the gray loop in Fig. 5a. Above the Néel temperature of Mn, 107 K, both shell and core are in a paramagnetic state (Fig. 5b). Decreasing the temperature below 107 K will result in the AFM ordering of Mn, while the shell remains random (Fig. 5c). As the temperature is lowered below 60 K, the uncompensated surface spins play an increasingly important role. After lowering the temperature of nanosized Mn powders to 5 K, in the FC case, the spins on the surface of the Mn(O)

should lie almost parallel to each other along the field direction (Fig. 5e). With the decreased field strength, the surface spin becomes disordered again (Fig. 5d). After the magnetic field is reversed, the spins on the Mn(O) surface start to rotate in the opposite direction. Due to the strong surface anisotropy of surface spins, a microscopic torque will occur for the surface spins of the Mn(O), trying to keep them in their original positions. Therefore, the magnetic field required to completely reverse the magnetization in the surface spins will be higher than that in normal state, i.e., an extra magnetic field will be required to overcome the microscopic torque exerted by the spins in the AFM. As a result, the coercive field in the negative field branch increases (Fig. 3). Conversely, when the magnetic field is reversed back to positive values, the rotation of surface spins along the initial direction will be easier than in the opposite direction, since the interaction with the spins in the AFM will now favour the magnetization reversal, i.e., the AFM will exert a microscopic torque in the same direction as the applied magnetic field (Fig. 5h). Therefore, the coercive field in the positive field branch will be reduced. The total effect will be a shift of the hysteresis loop along the magnetic field axis, H_e. Therefore, the surface spins play an important role in the considered system.

4. Conclusions

By means of milling Mn flakes in pure ethyl alcohol followed by homogenization, the nanosized Mn powders were fabricated. The X-ray diffraction measurement reveals its single-phase character, besides the broadening of diffraction peaks. The ZFC and FC magnetizations exhibit a large irreversibility with the onset of about 60 K. The fit of the Curie-Weiss law reveals a strong AFM interaction in the considered system. A large coercive field and shifted hysteresis loops, i.e. H_e = 83.6 kA/m, are observed at 5 K, after cooling in a 2 T field. The analysis of a simple phenomenological model illustrates that surface anisotropy plays an important role in the large exchange bias field of the considered system.

References

[1] IBRAHIM M.M., DARWISH S., SEEHRA M., Phys. Rev. B, 51 (1995), 2955.
[2] GIDER S., AWSCHALOM D.D., MANN S., CHAPARALA M., Science, 268 (1995), 77.
[3] MISHRA S.R., DUBENKO I., LOSOBY J., GHOSH K., KHAN M., ALI N., J. Nanosci. Nanotechnol., 5 (2005), 2076.
[4] MAKHLOUF S.A., AL-ATTAR H., KIDAMA R.H., Solid State Commun., 145 (2008), 1.
[5] BODKER F., HANSEN M.F., BENDER K.C., MORUP S., J. Magn. Magn. Mater., 221 (2000), 32.
[6] MEIKLEJOHN W.H., BEAN C.P., Phys. Rev., 102 (1965), 1314.
[7] PUNNOOSE A., MAGNONE H., SEEHRA M.S., BONEVICH J., Phys. Rev. B, 64 (2001), 174420.
[8] DEMANGEAT C., PARLEBAS J.C., Rep. Prog. Phys., 65 (2002), 1679.
[9] DONG X.L., ZHANG Z.D., ZHAO X.G., CHUANG Y.C., JIN S.R., SUN W.M., J. Mater. Res., 14 (1999), 1782.

[10] NEEL L., *Low Temperature Physics*, Gordon and Beach, New York, 1962.
[11] MORALES M.A., SKOMSKI R., FRITZ S., SHELBURNE G., SHIELD J.E., YIN M., O'BRIEN S., LESLIE -PELECKY D.L., Phys. Rev. B, 75 (2007), 134423.
[12] MAKHLOUF S.A., J. Magn. Magn. Mater., 246 (2002), 184.
[13] PUNNOOSE A., SEEHRA M.S., J. Appl. Phys., 91(10) (2002), 7766.
[14] KODAMA R.H., MAKHLOUF S.A., BERKOWITZ A.E., Phys. Rev. Lett., 79 (1997), 1393.
[15] KODAMA R.H., BERKOWITZ A.E., Phys. Rev. B, 59 (1999), 6321.
[16] REDDY B.V., DEEVI S.C., REUSE F.A., KHANNA S. N., Phys. Rev. B, 64 (2001), 132408.
[17] NOGUES J., SORT J., LANGLAIS V., SKUMRYEV V., SURINACH S., MUNOZ J.S., BARO M.D., Physics Report, 422 (2005), 65.

Received 1 June 2008
Revised 20 August 2008